First Demonstration of Ultra-Miniaturized, High-Performance Filters on Alumina Ribbon Ceramic Substrates for 5G Applications

Nahid Aslani-Amoli[#], Fuhan Liu[#], Madhavan Swaminathan[#], Cheng-Gang Zhuang[*], Nikolay Z. Zhelev[*], Seong-Ho Seok[*], Cheolbok Kim[*]

[#]3D Systems Packaging Research Center, School of ECE & MSE, Georgia Institute of Technology, USA

[*]Corning Incorporated, USA

aslani@gatech.edu

***Abstract* — This paper reports the first demonstration of ultra-thin, ultra-miniaturized filters with footprint smaller than $0.65\lambda_0 \times 0.16\lambda_0 \times 0.009\lambda_0$ fabricated on Alumina Ribbon Ceramic substrate operating at the frequency of 28-GHz band for 5G and mm-wave applications. A newly developed substrate material technology by Corning, Alumina Ribbon Ceramic can be utilized for realizing ultra-miniaturized, high-performance passive components due to its high dielectric constant and very low loss tangent. To show the effectiveness of Alumina Ribbon Ceramic for such applications, three bandpass filter (BPF) topologies, namely edge-coupled, interdigital and hairpin, and semi-lumped elliptical low-pass filter (LPF) topologies were modeled, designed, and fabricated on an 80-µm-thick Alumina Ribbon Ceramic metallized on both sides using a Semi-Additive Patterning (SAP) process. The performance of filters was characterized in the frequency range of 14-40 GHz using a vector network analyzer (VNA). In addition to exhibiting excellent agreement between the simulated and measured results of Alumina Ribbon Ceramic-based filters, their superiority is demonstrated through comparisons with those reported in the literature on other substrates in terms of performance and size. It is also highlighted that an insertion loss less than 1.3 dB is achieved for all filters.**

***Keywords* — Alumina Ribbon Ceramic, bandpass filter, 5G and mm-wave, hairpin, interdigital, low-pass filter, semi-additive process.**

I. Introduction

Increasing demands for higher data-rates are transforming the wireless communication systems from 4G LTE to 5G where millimeter-wave (mm-wave) frequencies are used to serve end-users. To meet the stringent requirements pertaining to 5G wireless systems, miniaturized and efficient components and modules are required to be developed to address design complexities posed in mm-wave frequencies. Radio frequency (RF) filters as one of the fundamental building blocks in 5G wireless communication systems are widely utilized in smart mobile phones [1]. The traditional filtering technologies used in 4G LTE such as surface acoustic wave (SAW) and bulk acoustic wave (BAW) as off-chip approaches cover a range of frequencies up to 6 GHz, having small sizes and good performance. However, their applications in mm-wave frequencies cause issues in terms of performance and size. Despite good performance, waveguide and cavity filters are bulky in size which is not a desirable attribute at mm-wave frequencies. On-chip filters using semiconductor technologies have small footprint at mm-wave frequencies but suffer from major performance issues regarding Q-factor, loss, and noise figure [2]. The strict filtering requirements like low in-band insertion loss and high out-of-band rejection along with miniaturization required in mm-wave region pose unique challenges to filter designers from the standpoint of size, performance, substrate selection, and impact of fabrication tolerances [3]. Therefore, new filter designs using innovative substrate technologies should be explored to meet the demanding requirements governing 5G filters. Showcased first at 2019 Ceramic Expo., Alumina Ribbon Ceramic [4] offers a nice opportunity for realizing ultra-miniaturized, high-performance passive devices on ultra-thin substrate material. Given its outstanding electrical properties, the application of Alumina Ribbon Ceramic is investigated in this paper for demonstrating the low-pass and bandpass filters on an 80-µm-thick Alumina Ribbon Ceramic substrate for 28-GHz US band (24.5-29.5 GHz) with a fractional bandwidth of 18.52%. Its higher dielectric constant combined with very low loss tangent (and high thermal conductivity) can help achieve highly miniaturized filters while having low insertion loss in the passband as required in 5G systems. As off-chip filters are desired in mm-wave frequency range, ultra-thin Alumina Ribbon Ceramic can be used as the core substrate for filter realizations either for embedding them into the package or making them stand-alone as integrated passive devices (IPDs) [5]. The remainder of this paper is structured as follows. Section II presents the design methodology of filters along with the material stack-up for their demonstration. The fabrication process of filters using semi-additive patterning (SAP) process is explained in Section III, followed by characterization results of filters, their model-to-hardware correlation and comparison with similar filters reported in the literature, provided in Section IV. Finally, Section V concludes the paper.

II. Filter Designs

The material stack-up used for fabrication of filters is shown in Fig. 1(a), where an 80-µm-thick Alumina Ribbon Ceramic is considered as a core substrate. According to [4], the measured dielectric constant and loss tangent of the Alumina Ribbon Ceramic based on Fabry-Perot open cavity from 10 GHz to 60 GHz are ~10 and ~0.0001, respectively. The diameter of the through-alumina via (TAV) is designed to be 40 µm which gives an aspect ratio of 2 in the 80-µm-thick Alumina Ribbon Ceramic and the via pitch is twice the via diameter [4]. The targeted copper thickness in the filter design process is chosen to be 6 µm. Two filter types, LPF and BPF, are designed to operate in the 28-GHz band. Due to its sharp roll-off at the cut-off frequency, semi-lumped elliptical LPF is selected over the Butterworth and Chebyshev LPF prototypes for the LPF demonstration on Alumina Ribbon Ceramic. For this purpose, after determining the filter order based on the desired attenuation in the stopband, the *g*-values corresponding to the LPF prototype with an elliptical response, shown in Fig. 1(b), are selected. By scaling the *g*-values to the desired impedance and frequency, the values of inductors and capacitors are calculated with the following equation [6]:

$$L_i = \frac{1}{2\pi f_c} Z_0 g_{Li} \text{ , } C_i = \frac{1}{2\pi f_c} \frac{1}{Z_0} g_{Ci} \tag{1}$$

where f_c is the cut-off frequency of LPF, Z_0 is the input/output terminal impedance (usually 50 Ω), and g_{Li} and g_{Ci} are *g*-values of the inductors and capacitors, respectively. For microstrip realization, all inductors and capacitors are implemented using high-impedance lines and low-impedance lines, respectively. The physical length of these lines corresponding to the *L* and *C* elements are calculated using following equations [6]:

$$l_{Li} = \frac{\lambda_{gL}(f_c)}{2\pi} arcsin\left(2\pi f_c \frac{L_i}{Z_{0L}}\right) \tag{2}$$

$$l_{Ci} = \frac{\lambda_{gC}(f_c)}{2\pi} arcsin(2\pi f_c Z_{0C} C_i) \tag{3}$$

where $\lambda_{gL}(f_c)$ and $\lambda_{gC}(f_c)$ are guided wavelengths at the cut-off frequency related to *L* and *C*, respectively and $Z_{0L}(> Z_0)$ and $Z_{0C}(< Z_0)$ are the characteristic impedances set for the high-impedance and low-impedance lines as 85.12 Ω and 17.35 Ω, respectively. In the design process, the minimum line width related to Z_{0L} was set to 14 µm to alleviate the impact of process variations on the filter response.

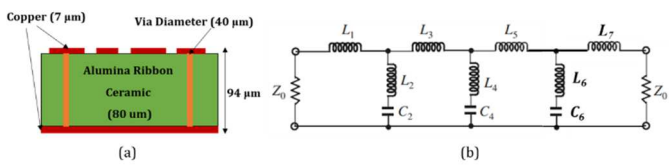

Fig. 1. (a) Material stack-up for fabrication of filters. (b) The seventh order elliptic-function, lumped-element LPF prototype.

Three different topologies, i.e., edge-coupled, hairpin, and interdigital are considered for the BPF demonstration on Alumina Ribbon Ceramic. Both edge-coupled and hairpin BPFs use half-wavelength ($\lambda/2$) resonators, open-circuited at both ends. However, the interdigital BPF utilizes resonators of length $\lambda/4$, with one end short-circuited and the other open-circuited, in alternating fashion. For the resonator length, λ is the wavelength in Alumina Ribbon Ceramic material calculated at the center frequency of BPF [7]. All BPF topologies are designed based on 0.01-dB-ripple Chebyshev polynomial LPF prototype g-values with design procedure details described in [6]–[8]. All designed filter topologies were simulated and optimized in ANSYS HFSS v19.3 [9] over the frequency range of 14-40 GHz, given the design parameters listed in Table 1 based on 5G requirements [3].

Table 1. Design parameters for 28-GHz band filters on Alumina Ribbon Ceramic substrate

Parameter	**Objectives & Goal**	
	LPF	BPF
Cut-off frequencies	29.5 GHz	24.5 and 29.5 GHz
Insertion loss at cut-off frequencies	<2 dB	<2.5 dB
30-dB attenuation point to band-edge ratio	<1.24	<1.20

To characterize the fabricated filters, the conductor-backed coplanar waveguide (CBCPW) to microstrip transitions were designed and used at both ends of all filters. These probe pads are compatible with the pitch of the Cascade MicroTech probe which is at 200 µm.

III. Fabrication Process of Filters

The designed filters are fabricated using SAP process [10] where the process starts with a bare Alumina Ribbon Ceramic panel with laser-drilled TAVs. Then, a seed layer of Titanium/Copper (50nm/150nm) is deposited on both sides of the panel. After laminating a 30-µm-thick dry-film photoresist (DFR) and TAV alignment, the mask is exposed on the panel, followed by DFR development and electrolytic plating to achieve the desired copper thickness. At the end, the DFR is stripped, and the deposited seed layer (Ti/Cu) is etched to obtain the final filter circuits. After inspecting the fabricated panel using Zeta Optical Profilometer, the measured copper thickness was found to be 7 µm and diameters of taper shaped TAVs were 48 µm and 22 µm on the entry and exit sides, respectively. Moreover, the observed variation in the width of high-impedance lines for fabricated LPFs is ~1 µm. For all BPF topologies, the resonator width exhibits a maximum variation of ~2 µm, leading to a decrease in spacings between resonators. In summary, fabrication tolerances are within a very small region which indicates the high accuracy of fabrication process, required for filter realizations at mm-wave frequencies. The fabricated filters on Alumina Ribbon Ceramic are depicted in Fig. 2 where each filter is surrounded by a ground via wall to ensure better grounding and to isolate

it from adjacent structures on the panel. The filters are simulated in ANSYS HFSS using the measured dimensions to examine the model-to-hardware correlation in the next section.

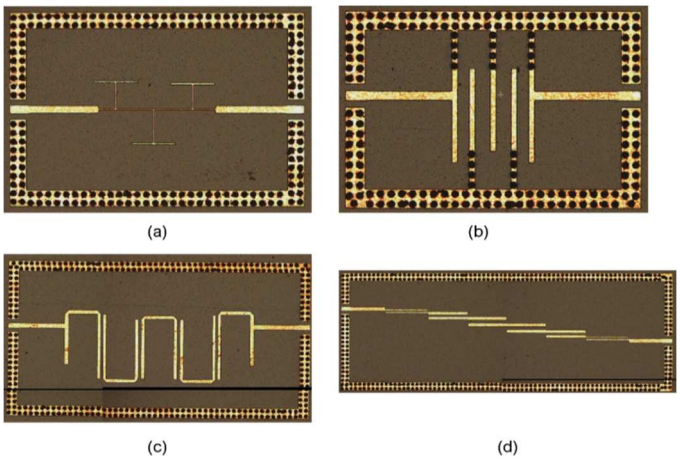

Fig. 2. Fabricated filters on Alumina Ribbon Ceramic for 28-GHz band: (a) seventh order LPF; (b) fifth order interdigital BPF; (c) fifth order hairpin BPF; (d) fifth order edge-coupled BPF.

IV. Measurement Results and Filter Comparisons

The fabricated filters were measured using an Agilent E8363B VNA in the frequency range of 14-40 GHz with ACP40 GSG probes after performing the short-open-load-through (SOLT) calibration. Six coupons of each filter were measured on the fabricated panel along with the thru-reflect-line (TRL) structures to de-embed the measured S-parameters of filters. Fig. 3 shows the comparison between the simulated and measured insertion loss (S_{21}) and return loss (S_{11}) results of fabricated filters. As seen, an excellent model-to-hardware correlation is achieved for all filters. For the LPF, the measured insertion loss at 29.5 GHz is 1.27 dB and 30-dB attenuation point to band-edge ratio is 1.18 which meet the design specifications listed in Table 1. Also, good impedance matching is observed for this filter. In Fig. 3, despite a slight increase in the bandwidth of all BPFs due to a slight decrease in the resonator spacings, the measured insertion loss at the cut-off frequencies for all BPFs is less than 2 dB and the passband return loss is better than 20 dB, showing an excellent impedance match. In edge-coupled, hairpin and interdigital BPFs, the measured insertion loss at the center frequency (27 GHz) is 1.3 dB, 1.11 dB, and 0.77 dB, respectively. Moreover, 30-dB attenuation point to band-edge ratio for these BPFs are 1.18, 1.19, and 1.11, respectively, which meet the design requirements very well. In short, all measured filters exhibit low insertion loss, good impedance match and high selectivity (30-dB attenuation point to band-edge ratio of 1.2 maximum). From measured dimensions of fabricated filters, the physical size of each filter is obtained, and the corresponding electrical size is calculated by normalizing the physical size to the free-space wavelength at 28 GHz which is 10.71 mm. Table 2 presents both physical and electrical sizes of fabricated filters on Alumina Ribbon Ceramic where the footprint of all filters is smaller than $0.65\lambda_0 \times 0.16\lambda_0 \times 0.009\lambda_0$, with a total height of 94 µm. A comprehensive survey was conducted in the literature to evaluate the demonstrated filters on Alumina Ribbon Ceramic for 28-GHz band as compared to similar filters. The results shown in Table 3 indicate that the realized filters on Alumina Ribbon Ceramic demonstrate the smallest footprint and outperform similar filters in terms of performance as well. Based on Table 3, a size reduction up to 85% is achieved for BPFs fabricated on Alumina Ribbon Ceramic, making them good candidates for applications like in small cells.

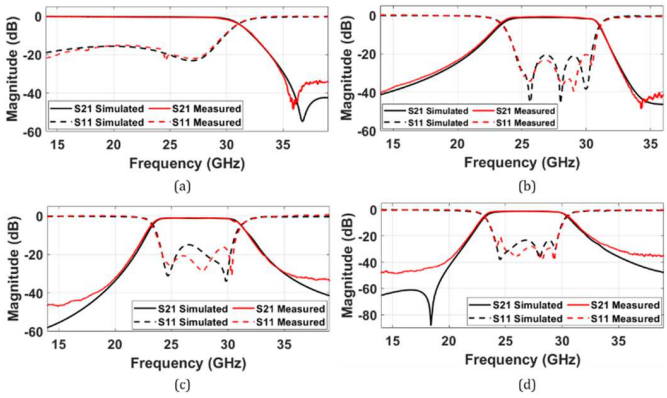

Fig. 3. Correlation between measured and simulated results of fabricated filters on Alumina Ribbon Ceramic for 28-GHz band: (a) seventh order LPF; (b) fifth order interdigital BPF; (c) fifth order hairpin BPF; (d) fifth order edge-coupled BPF.

Table 2. Physical and electrical sizes of fabricated filters on Alumina Ribbon Ceramic substrate

28-GHz band Filters	**Physical Size (mm^3)**	**Electrical Size $(\lambda_0)^3$**
7th order LPF	$1.75 \times 0.79 \times 0.094$	$0.16 \times 0.07 \times 0.009$
5th order interdigital BPF	$1.29 \times 1.72 \times 0.094$	$0.12 \times 0.16 \times 0.009$
5th order hairpin BPF	$2.89 \times 1.07 \times 0.094$	$0.27 \times 0.10 \times 0.009$
5th order edge-coupled BPF	$7 \times 0.63 \times 0.094$	$0.65 \times 0.06 \times 0.009$

V. Conclusion

Demonstration of ultra-miniaturized, high-performance filters with footprint smaller than $0.65\lambda_0 \times 0.16\lambda_0 \times 0.009\lambda_0$ on an ultra-thin Alumina Ribbon Ceramic substrate is presented in this work for 5G and mm-wave applications. Four topologies of two filter types, LPF and BPF, are designed, optimized, and fabricated on an 80-µm-thick Alumina Ribbon Ceramic using SAP process for 28-GHz band. Apart from excellent agreement between simulations and measurements, fabricated filters on Alumina Ribbon Ceramic stand out among similar filters reported in the literature from the standpoint of size, passband insertion loss and out-of-band rejection. It demonstrates promising applications of Alumina Ribbon Ceramic for realizing highly efficient passive components in 5G and mm-wave frequency bands. The demonstrated filters on Alumina Ribbon Ceramic in 39-GHz EU band (37-43.5 GHz) and 5G NR bands will be presented in the future works.

Table 3. Comparison of the fabricated filters on Alumina Ribbon Ceramic substrate with the literature

Ref. filter - order	**Type**	***f₀* (GHz) – FBW (%)**	**Insertion loss**	**Electrical size $(\lambda_0)^3$**	**Size reduction (%)-Ref.**
[11]-4	Stacked SIW on LTCC	27.95-3.7%	2.8 dB	$0.57 \times 0.30 \times 0.04$	-
[12]-3	edge-coupled on Teflon	27.85-4.7%	4 dB	$0.43 \times 0.23 \times 0.024$	-
[5] - 5	Hairpin BPF on ABF GL102	27-18.52%	-	$0.43 \times 0.19 \times 0.018$	-
[3] - 5	Interdigital BPF on ABF GL102	27-18.52%	2.6 dB	$0.29 \times 0.21 \times 0.018$	-
This work - 5	Hairpin BPF on Alumina Ribbon Ceramic	27-18.52%	1.11 dB	$0.27 \times 0.10 \times 0.009$	83.5%-[5]
This work - 5	Interdigital BPF on Alumina Ribbon Ceramic	27-18.52%	0.77 dB	$0.12 \times 0.16 \times 0.009$	84.2%-[3]
This work - 5	edge-coupled BPF on Alumina Ribbon Ceramic	27-18.52%	1.3 dB	$0.65 \times 0.06 \times 0.009$	85.2%-[12]

ACKNOWLEDGMENT

This work was supported by Corning Incorporated and the industry consortium at Georgia Tech's 3D Systems Packaging Research Center (PRC). We acknowledge the contribution of Colin Daly, Scott Pollard, Scott Silence, Karan Mehrotra and Gordon Brown for Corning Incorporated for supporting and establishing this research activity.

REFERENCES

[1] S. Mahon, "The 5g effect on rf filter technologies," *IEEE Transactions on Components, Packaging, and Manufacturing Technology*, vol. 30, no. 4, pp. 494–499, Nov. 2017.

[2] DOEEET Blog, (2020) Approaching the 5g mmwave filter challenge, [Online]. Available: https://www.doeeet.com/content/eee-components/rf-mw/approaching-the-5g-mmwave-filter-challenge/

[3] M. Ali, F. Liu, A. Watanabe, P. M. Raj, V. Sundaram, M. M. Tentzeris, and R. R. Tummala, "Miniaturized high-performance filters for 5G small-cell applications," *IEEE 68th Electronic Components and Technology Conference (ECTC)*, pp. 1068–1075, May 2018.

[4] C. Zhuang, Y. Wang, L. Cai, J. Markley, H. Vanselous, N. Zhelev, S. -H. Seok, L. Kester, and M. Badding, "Flexibility matters: high purity, thin, flexible alumina ribbon ceramic," *Ceramic & Glass Manufacturing*, vol. 1, no. 4, Sep. 2020.

[5] M. Ali, F. Liu, A. Watanabe, P. M. Raj, V. Sundaram, M. M. Tentzeris, and R. R. Tummala, "First demonstration of compact, ultra-thin low-pass and bandpass filters for 5G small-cell applications," *IEEE Microwave and Wireless Components Lett.*, vol. 28, No. 12, pp. 1110–1112, Dec. 2018.

[6] J.-S. G. Hong, and M. J. Lancaster, *Microstrip Filters for RF/Microwave Applications*, vol. 167. Hoboken, NJ, USA: Wiley, 2004.

[7] Z. Awang, *Microwave Systems Design*, Singapore: Springer, 2014.

[8] J. S. Wong, "Microstrip tapped-line filter design," *IEEE Transactions on Microwave Theory and Techniques*, vol. 27, no. 1, pp. 44–50, Jan. 1979.

[9] ANSYS. ANSYS HFSS Ver. 2019.3. Accessed: Jul. 15, 2020. [Online]. Available: http://www.ansys.com

[10] H. Akahoshi, M. Kawamoto, T. Itabashi, O. Miura, A. Takahashi, S. Kobayashi, M. Miyazaki, T. Mutoh, M. Wajima, and T. Ishimaru, "Fine line circuit manufacturing technology with electroless copper plating," *IEEE Transactions on Components, Packaging, and Manufacturing Technology – Part A*, vol. 18, no. 1, pp. 127–135, Mar. 1995.

[11] K. S. Chin, C. C. Chang, C. H. Chen, Z. Guo, D. Wang, and W. Che, "LTCC multilayered substrate-integrated waveguide filter with enhanced frequency selectivity for system-in-package application," *IEEE Transactions on Components, Packaging, and Manufacturing Technology*, vol. 4, no. 4, pp. 664–672, Apr. 2014.

[12] Y. M. Yan, Y. T. Chang, H. Wang, R. B. Wu, and C. H. Chen, "Highly selective microstrip bandpass filters in ka-band," *32nd European Microwave Conference*, pp. 1-4, Sep. 2002.